

Article

Bearing-Based Distributed Formation Control of Unmanned Aerial Vehicle Swarm by Quaternion-Based Attitude Synchronization in Three-Dimensional Space

Muhammad Baber Sial ^{1,*}, Yuwei Zhang ¹, Shaoping Wang ^{1,2,3}, Sara Ali ^{4,5}, Xinjiang Wang ^{1,2,3}, Xinyu Yang ⁶, Zirui Liao ¹ and Zunheng Yang ¹

¹ School of Automation Science and Electrical Engineering, Beihang University, Beijing 100191, China

² Beijing Advanced Innovation Center for Big Data-Based Precision Medicine, Beihang University, Beijing 100191, China

³ Ningbo Institute of Technology, Beihang University, Ningbo 315800, China

⁴ School of Mechanical and Manufacturing Engineering, National University of Sciences and Technology, Islamabad 44000, Pakistan

⁵ Human-Robot Interaction (HRI) Lab, School of Interdisciplinary Engineering & Science (SINES), Islamabad 44000, Pakistan

⁶ School of Energy and Power Engineering, Beihang University, Beijing 100191, China

* Correspondence: babersial@buaa.edu.cn



Citation: Sial, M.B.; Zhang, Y.; Wang, S.; Ali, S.; Wang, X.; Yang, X.; Liao, Z.; Yang, Z. Bearing-Based Distributed Formation Control of Unmanned Aerial Vehicle Swarm by Quaternion-Based Attitude Synchronization in Three-Dimensional Space. *Drones* **2022**, *6*, 227. <https://doi.org/10.3390/drones6090227>

Academic Editors: Xiwang Dong, Mou Chen, Xiangke Wang and Fei Gao

Received: 27 July 2022

Accepted: 26 August 2022

Published: 30 August 2022

Publisher's Note: MDPI stays neutral with regard to jurisdictional claims in published maps and institutional affiliations.



Copyright: © 2022 by the authors. Licensee MDPI, Basel, Switzerland. This article is an open access article distributed under the terms and conditions of the Creative Commons Attribution (CC BY) license (<https://creativecommons.org/licenses/by/4.0/>).

Abstract: Most of the recent research on distributed formation control of unmanned aerial vehicle (UAV) swarms is founded on position, distance, and displacement-based approaches; however, a very promising approach, i.e., bearing-based formation control, is still in its infancy and needs extensive research effort. In formation control problems of UAVs, Euler angles are mostly used for orientation calculation, but Euler angles are susceptible to singularities, limiting their use in practical applications. This paper proposed an effective method for time-varying velocity and orientation leader agents for distributed bearing-based formation control of quadcopter UAVs in three-dimensional space. It combines bearing-based formation control and quaternion-based attitude control using undirected graph topology between agents without the knowledge of global position and orientation. The performance validation of the control scheme was done with numerical simulations, which depicted that UAV formation achieved the desired geometric pattern, translation, scaling, and rotation in 3D space dynamically.

Keywords: formation control; UAV swarm; quadrotor UAVs; VTOL UAVs; attitude synchronization; orientation estimation; bearing-based formation control

1. Introduction

Nature has always inspired many great scientific triumphs and countless feats in the advancement of technology. Observation of natural formations of creatures such as a flock of birds, a school of fish, and formations of ants makes us realize that each entity in the formation controls its place in the formation just by aligning itself with respect to each other's bearing angle without knowledge of its global position or orientation. The same is true for aerobic displays of piloted jet aircrafts in formation flying, where each aircraft is flown at a specific angle with other aircrafts of the formation. Design and control of distributed agent formations have become a keystone to solving multifarious complex applications such as coordination of mobile robots [1], satellite formation flying [2], and search and rescue [3]. A group or formation of UAVs, also referred to as a UAV swarm, has received compelling attention in military and civilian applications [4–6]. The process in which a group of agents obtains and maintains a predetermined geometric shape in space is called formation control [7].

UAV formations are all set to become one of the most essential tools for future military and civilian operations [8]. Formation control strategies, in which spatial constraints are defined among agents, are a powerful instrument in multi-robot systems [9]. Many kinds of consensus algorithms related to formation control for multi-agent systems can be found in the literature, mainly categorized as leader–follower [10], virtual structure [11], and potential field methods [12]. The leader–follower configuration is a widespread technique in formation control literature [13]. This configuration is ideal yet nontrivial in the case of distributed multi-agent systems, where a central controller such as a ground station is not present to centrally control all the agents. The leader follows a specific path or reference trajectory while all the followers are bound to adjust their position with respect to the leader. Because only knowledge about neighboring robots is required to define the formation, the leader–follower architecture best fits distributed schemes by enabling formation control relative to agent poses [14].

The current formation control methods, as per sensed and controlled variables, can be categorized into three groups: (1) position-based, (2) distance-based, and (3) bearing-based [9]. Position-based methods are currently most employed because they utilize the fact that each agent in the formation can obtain its position with respect to the global coordinate frame [15–17]. This means the agents rely on the global positioning system (GPS) or other related sensor information, forcing them to rely on external information to help conform themselves in a formation. However, in many situations, such as urban indoor or subterranean environments, the external signals cannot be obtained and position accuracy is uncertain, making it inadvisable to rely on such information. It is preferred to rely on an agent's onboard sensors rather than external sources for measurements. Trinh et al. [18,19] have verified that distance-based rigid formation control could not achieve global stability; furthermore, flip ambiguities commonly occur in distance-rigid graphs [20]. Additionally, compared to other approaches, the bearing-only approach has some advantageous features, such as relying less on the sensing ability of each robot [21]. The problem of bearing-based formation control of non-holonomic robots was considered by Li et al. [21] in 3D space using the Euler–Lagrange model using Euler angles to express 3D rotations of agents. Initial research on bearing-based formation control [22,23] was restricted to 2D space and primarily intended to control the bearing between agents to achieve the desired formation configuration. As per the proposed bearing rigidity theory, an almost globally stable control law was proposed for the single integrator robot with or without the inertial reference frame [24]. It is also important to mention that most of the reported research [24–26] has modeled their agents as a single or double integrator with randomly controlled velocity and acceleration. Using bearing rigidity-based control architecture also uniquely determines the formation's shape [24]. Additionally, it is paramount that orientation dynamics are independent of the position dynamics but not the other way around [24]. The bearing can also be calculated by employing the agent's onboard cameras [27] or vision sensors and sensor arrays [28,29].

Complete formation maneuver control and time-varying formation control using bearing-only measurements have not been realized yet [21]. Bearing rigidity theory to solve nonlinear robotic systems has generally only used the Euler–Lagrange model [21], where systems subjected to non-holonomic constraints are discussed. Quaternions are preferred over Euler angles because the latter are prone to gimbal lock when two out of three axes align during interpolation. Simple linearization using Euler angles overcompensates the errors in environments susceptible to unknown errors. Furthermore, if the inclination in disturbances is too large, the linear conditions are not met. However, using quaternions instead of Euler angles, even hard inclinations can also be sustained. Robustness against external disturbances is also a key factor for preferences of quaternions over Euler angles. Furthermore, it has also been observed that conversion of quaternions into a matrix is also efficient. Their mathematical simplicity comes from the fact that for modeling rigid body dynamics, no trigonometric functions are required [30]. As per the reviewed literature, directed graph topology takes less of a toll on the overall computation complexity of the

formation but is not as robust as undirected graphs. In undirected graphs, bidirectional control of relative bearing measurements makes the formation more robust.

Motivated by the above observations, the significance of this article is such that we proposed a singularity-free novel quaternion-based relative attitude synchronization control scheme to reinforce undirected bearing-based control of a UAV swarm. Each agent's relative attitude and bearing were measured locally with its neighbor; hence, the dependence on the global coordinate frame was eliminated. The proposed approach validated its effectiveness on time-varying velocity and time-varying orientation leader agents in 3D space.

The main theoretical contributions of this article are:

1. A novel cascaded approach for distributed formation control of quadcopter UAVs was presented, consisting of an undirected bearing-based controller and a quaternion-based attitude synchronization controller working together in unison.
2. The distributed attitude synchronization and bearing-based formation control law were designed for 3D formation control as compared to [22,23], which have only designed bearing-based controllers for 2D space. Moreover, the proposed scheme uses quaternion-based attitude control, which is much more robust than research that has used Euler angles such as [21,31].
3. This work investigated and implemented the distributed formation control for time-varying velocity and time-varying orientation leader agents, which has not been accomplished yet in the domain of bearing-based formation control as compared to [21,31,32].
4. We designed our control method based on dynamic models of UAVs and undirected graph topology, a more robust technique as compared to [21,24,31], which only have used directed graph communications and kinematic models. The practical validation of the model was done using numerical simulations in MATLAB.

The remainder of this paper is organized as follows. In Section 2, preliminaries and problem formulation are given. Section 3 presents the system model and proposed control design. Section 4 covers the simulations and analysis, whereas discussion and the conclusions are drawn in Sections 5 and 6, respectively.

2. Preliminaries

In this section, we discuss some necessary background concepts about quaternions, the UAV quadcopter dynamical model, graph theory, and bearing rigidity theories that form a basis for problem formulation and design of our proposed control scheme.

2.1. Quaternions

This section briefly covers the mathematical background of quaternions, which are four-dimensional algebraic constructs that extend the concept of complex numbers. While quaternions are less comprehensible than Euler angles, quaternions lead to more efficient and accurate computation of rotations [33]. A quaternion is expressed formally as $q = q_0 + q_1i + q_2j + q_3k$, where q_0 represents the real part or the scalar part and $q_1i + q_2j + q_3k$ represents the vector part in \mathbb{R}^3 . Similarly, a pure quaternion's real part is zero. The conjugate of a quaternion is $q^* = q_0 - q_1i - q_2j - q_3k$, whereas its norm is

$$\|q\| = \sqrt{q \otimes q^*} = \sqrt{q_0^2 + q_1^2 + q_2^2 + q_3^2} \quad (1)$$

The norm is calculated by taking the Kronecker product of a simple quaternion and its conjugate. Similarly, the quaternion inverse can be given by

$$q^{-1} = \frac{q^*}{\|q\|} \quad (2)$$

The quaternion conjugate can also be expressed as $q^* = q_0 - q_1i - q_2j - q_3k$ and similarly, the quaternion inverse can be obtained by $q^{-1} = \frac{q^*}{\|q\|}$ hence $q^{-1} = q^*$. We assumed that only unit quaternions are used for quadrotor attitude representation for this work. Rotation from one coordinate frame A to another coordinate frame B can be expressed by conjugate operation; a quaternion expresses a rotation q_R with an added condition that its norm is equal to 1. Therefore, if q_A is a quaternion expressed in frame A, then the same quaternion can be expressed in frame B as:

$$q_B = q_R q_A q_R^* \tag{3}$$

We compute the multiplication of quaternions to change a coordinate frame

$$q_R q_A q_R^* = (q_0 + q_1i + q_2j + q_3k)(x_i + y_j + z_k)(q_0 - q_1i - q_2j - q_3k) \tag{4}$$

The product collected in one quaternion gives us

$$q_R q_A q_R^* = (x(q_0^2 + q_1^2 - q_2^2 - q_3^2) + 2y(q_1q_2 - q_0q_3) + 2z(q_0q_2 + q_1q_3))i + (2x(q_0q_3 + q_1q_2) + y(q_0^2 - q_1^2 + q_2^2 - q_3^2) + 2z(q_2q_3 - q_0q_1))j + (2x(q_1q_3 - q_0q_2) + 2y(q_0q_1 + q_2q_3) + z(q_0^2 - q_1^2 - q_2^2 + q_3^2))k \tag{5}$$

Quaternions in formation control circulated around simply using quaternions for representation of the orientation of each agent with respect to a global frame [34] or one of the other agents serving as an orientation reference [35]. As per the Euler theorem for rigid bodies [32], the rotation of a body around an axis in R^3 can be expressed in quaternions. The attitude of the i th quadrotor defined by the unit quaternion is given as

$$Q = \begin{bmatrix} \eta \\ \mathbf{q} \end{bmatrix} = \begin{bmatrix} \|e\| \sin \frac{\theta}{2} \\ \cos \frac{\theta}{2} \end{bmatrix} \tag{6}$$

where $\|e\|$ represents a unit axis in Euclidean space on which the agent is rotated, and θ is the magnitude of rotation. As the quaternion norm is equal to 1, it is used as the rotation operator. q represents the vector part and gives the magnitude of rotation, and η represents the scalar part and gives the axis of rotation. While some conventions also use the representation where the rotation is expressed later than the axis such as $Q = [\eta \quad \mathbf{q}]^T$, it is of less significance and varies from one method to another. The unit quaternion Q can also be transformed into its equivalent rotation matrix by the Rodrigues formula which is

$$R(Q) = (\eta^2 - \mathbf{q}^T \mathbf{q})I_3 + 2\mathbf{q}\mathbf{q}^T - 2\eta S(\mathbf{q})$$

$$S(\mathbf{q}) = \begin{pmatrix} 0 & -q_3 & q_2 \\ q_3 & 0 & -q_1 \\ -q_2 & q_1 & 0 \end{pmatrix} \tag{7}$$

where $S(\cdot)$ is the skew-symmetric matrix operator.

Quadcopter UAV Attitude Dynamics

Considering a swarm of n number of UAVs, the dynamics of the i th agent can be given as in [36].

$$\begin{aligned} \dot{p}_i &= v_i \\ m_i \dot{v}_i &= m_i g \hat{e}_3 - \Gamma_i R(Q_i)^T \hat{e}_3 \\ \dot{Q}_i &= \frac{1}{2} T(Q_i) \omega_i \\ J_i \dot{\omega}_i &= \tau - S(\omega_i) J_i \omega_i \end{aligned} \tag{8}$$

For $i \in N := \{1, 2, \dots, n\}$, p_i denotes the position, v_i denotes the velocity, m_i denotes the mass of the i th UAV, $Q_i = (q_i^T \quad \eta_i)^T$ is the agent's orientation, and $\omega_i = [\omega^x, \omega^y, \omega^z]^T \in R^3$ is the angular velocity denoted by the skew-symmetric matrix operator from R^3 to a matrix in $R^{3 \times 3}$. The positive scalar Γ denotes the total thrust

by all four rotors in the direction $\hat{e} = (0 \ 0 \ 1)^T$ unit vector in the body coordinate frame, and τ is the control input torque. $T(Q)$ can be given as

$$T(Q) = \begin{pmatrix} \eta I_3 + S(q) \\ -q^\top \end{pmatrix} \tag{9}$$

For a UAV leader–follower configuration, the relative attitude between the i th agent (leader) and j th agent (follower) expressed by the unit quaternion $Q_{ij} = (q_{ij}^\top \ \eta_{ij})^\top$ can be defined as

$$Q_{ij} = Q_j^{-1} \circ Q_i \tag{10}$$

The relative attitude between the two agents can be expressed as

$$\dot{Q}_{ij} = \frac{1}{2} T(Q_{ij}) \omega_{ij}, \quad T(Q_{ij}) = \begin{pmatrix} \eta_i I_3 + S(q_{ij}) \\ -q_{ij}^\top \end{pmatrix} \tag{11}$$

where ω_{ij} is the relative angular velocity of the i th agent’s body frame with respect to the j th agent’s body frame expressed in the i th agent’s body frame given as

$$\omega_{ij} = \omega_i - R(Q_{ij}) \omega_j \tag{12}$$

where the rotation matrix $R(Q_{ij})$ represents the rotation from the j th agent’s body frame to the i th agent’s body frame such as

$$R(Q_{ij}) = R(Q_i) R(Q_j)^\top \tag{13}$$

Figure 1 shows the representation of a UAV in the inertial reference frame O_W and the body-fixed frame O_B . Figure 1a shows a dynamic model of a quadrotor UAV in Euler angles and depicts the different actuator level entities affecting flight dynamics. Each of the four propellers rotates with an angular speed ω_i , producing thrust force F_i upwards and with opposite rotor spins. Figure 1b shows the quaternion representation of the same UAV in 3D space.

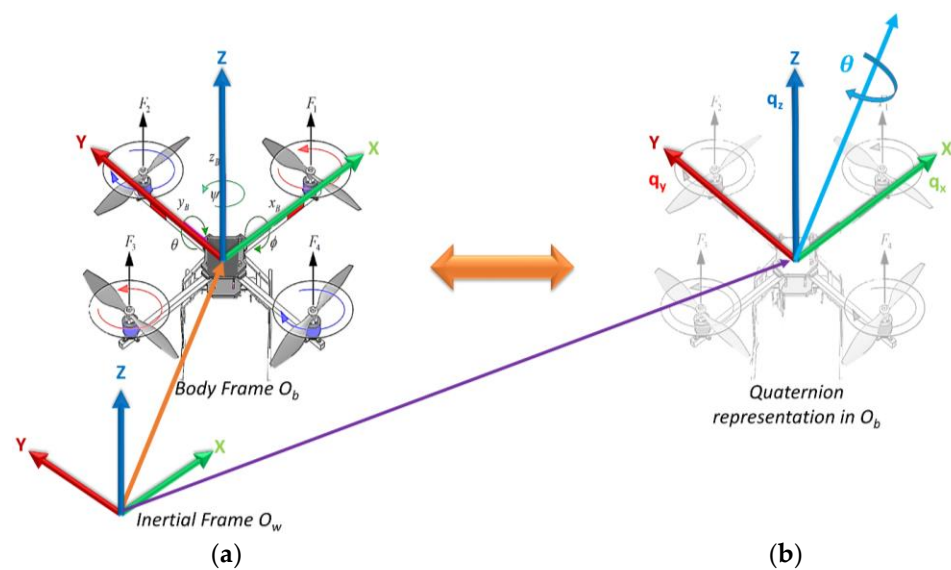


Figure 1. (a) UAV dynamical model expressed in inertial and body reference frames with Euler angles. (b) UAV model expressed with quaternions.

2.2. Graph and Bearing Rigidity Theories

Consider an individual UAV n in which ($n \geq 2$) can be considered as a swarm of UAVs. An undirected graph $G = (V, E)$ characterizes a dynamic undirected interaction network among multiple UAVs in the swarm representing a set of nodes $V = \{1, 2, \dots, n\}$ representing UAVs, and the interaction among UAVs is represented by a set of edges $E = \{e_{ij}: i = 1, 2, \dots, n, j \in N_i\}$, with the neighbor set N_i of UAVs. The graph is directed if $(v_i, v_j) \in E, (v_j, v_i) \notin E$ and undirected if otherwise.

It is problematic to inspect the distinctiveness of the formation shape determined by distance rigidity because the rank condition of infinitesimal distance rigidity cannot assure the formation shape to be unique [37]. However, in bearing rigidity theory, the rank condition and formation shape distinctiveness are considered adequate. In any coordinate frame, $p_i(t) = [p_i^x, p_i^y, p_i^z]^T \in R^3$ being the position of the i th UAV $C = [p_1^T, p_2^T \dots \dots p_n^T]^T \in R^3$ shows the configuration of the formation, and similarly, the desired configuration can be expressed as $C^* = [p_1^{*T}, p_2^{*T} \dots \dots p_n^{*T}]^T \in R^3$. A UAV formation, represented by (G, C) , is a blend of graph G and a configuration C , where every $v_i \in V$ is related to a position p_i in the configuration [38]. Therefore, for (G, C) , define

$$\begin{aligned} e_{ij} &\triangleq p_j - p_i \\ g_{ij} &\triangleq \frac{e_{ij}}{\|e_{ij}\|} \end{aligned} \tag{14}$$

where e_{ij} denotes an edge vector and g_{ij} represents a unit vector, which gives the bearing from p_j to p_i . This unit vector representation represents both the azimuth angle and altitude angle in R^3 . The objective of a UAV formation is to transform into a desired geometrical shape or final configuration by controlling the bearing constraints of its agents, where bearing constraints can be defined as

$$\beta_G = \left\{ \frac{g_{ij}^* = (p_j^* - p_i^*)}{\|p_j^* - p_i^*\|} (v_j, v_i) \in E \right\} \tag{15}$$

In a UAV swarm, the desired distance between two agents is given by $d_{21}^* = \|p_1^* - p_2^*\|$, while β_G is a set of bearing constraints, and the target position of the next agent can be defined as $p_2^* = p_1^* - d_{21}^* g_{21}^*$; here, d , p , and g represent distance, position, and bearing of the agents, respectively. Inspired by [37], an orthogonal projection operator $P_{g_{ij}}$ is introduced to geometrically project any vector at the orthogonal complement of x ; moreover, the $\text{Null}(P_{g_{ij}}) = \text{span}\{x\}$ and the eigenvalues of $P_{g_{ij}}$ are $\{0, 1^{(d-1)}\}$, such that for any vector $x > 0, x \in R^d (d \geq 2)$, the operator $P_{g_{ij}} : R^d \rightarrow R^{d \times d}$ is defined as

$$\begin{aligned} P_{g_{ij}} &\triangleq I_d - \left(\frac{x}{\|x\|}\right) \left(\frac{x}{\|x\|}\right)^T \\ P_{g_{ij}} &\triangleq I_3 - g_{ij} g_{ij}^T \end{aligned} \tag{16}$$

The orthogonal projection matrix provides an efficient way to define the parallel vectors in bearing rigidity theory. To define the target formation, we introduce a bearing Laplacian matrix as introduced in [24], which is

$$[B(G(p^*))]_{ij} = \begin{cases} 0_{d \times d}, & i \neq j, (i, j) \notin \varepsilon \\ -P_{g_{ij}}^*, & i \neq j, (i, j) \in \varepsilon \\ \sum_{k \in N_i} P_{g_{ik}}^*, & i = j, i \in V \end{cases} \tag{17}$$

This bearing Laplacian matrix B describes the inter-agent topology and bearings between agents. Similarly, the bearing Laplacian matrix can be explained as

$$B = \begin{bmatrix} B_{LL} & B_{LF} \\ B_{FL} & B_{FF} \end{bmatrix} \tag{18}$$

where every part can be explained as $B_{LL} \in \mathbb{R}^{dn_L \times dn_L}$, $B_{LF} \in \mathbb{R}^{dn_L \times dn_F}$, $B_{FL} \in \mathbb{R}^{dn_F \times dn_L}$, and $B_{FF} \in \mathbb{R}^{dn_F \times dn_F}$ is significant and useful, being symmetric positive semidefinite. We also need to ensure that the framework is unique and rigid; therefore, we employ the infinitesimal bearing rigidity theory introduced by [24]. This theory states that: if a framework (G, C) is infinitesimally rigid, it depicts two vital properties: (1) the positions of the vertices can be distinctively calculated up to a translational and a scaling factor, and (2) the configurations are infinitesimally bearing rigid in a d -dimensional space if and only if the bearing rigidity matrix satisfies: $\text{Null}(G_{ij}^B(C)) = \text{span}\{1_n \otimes I_d, p\}$ or

$$\text{rank}(G_{ij}^B(C)) = dn - d - 1 \tag{19}$$

where n number of agents in a swarm are expressed in \mathbb{R}^d , comprising dn coordinates, d specifying the centroid, and 1 specifying the scale and being subtracted, and if the resulting value is equal to the rank of $G_{ij}^B(C)$, it means that the formation is infinitesimal bearing rigid. Due to these two properties [24], infinitesimally bearing rigid configurations not only have unique geometric shapes but can also be mathematically inspected. The centroid and scale [38] can be defined as

$$\begin{aligned} c(p^*(t)) &= \frac{1}{n} \sum_{i=1}^n p_i^*(t) \\ s(p^*(t)) &= \sqrt{\frac{1}{n} \sum_{i=1}^n \|p_i^*(t) - c(p^*(t))\|^2} \end{aligned} \tag{20}$$

For bearing rigidity, it is vital to determine if two given bearings are equal; thus, the orthogonal projection operator provides an upfront approach. Figure 2 illustrates the difference between rigid and non-rigid graphs and shows the topology used in this work.

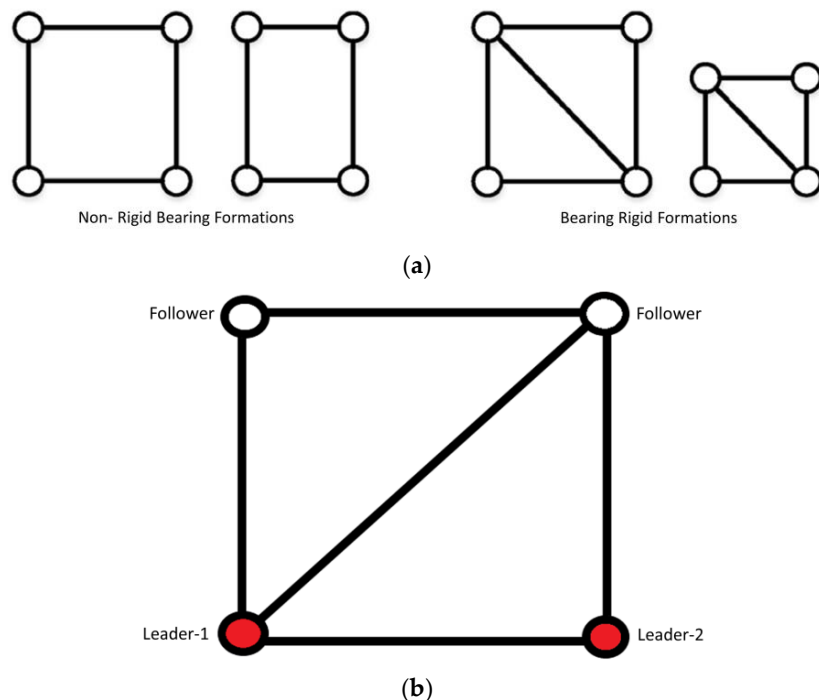


Figure 2. (a) Examples of non-rigid and rigid bearing formations. (b) Proposed Formation Topology.

2.3. Problem Formulation

We designed a cascaded model for formation control of a UAV swarm, considering the dynamic model of quadrotor UAVs. In the upper cascade, we gave the bearing-based law, and in the lower cascade, we designed the attitude synchronization controller that improves the performances of [21,24,31] by the use of quaternions instead of Euler angles. This complete cascaded structure was then used to simulate a UAV swarm’s translation, scaling, and rotation in 3D space.

We formulated the problem as follows.

Problem 1. Consider a UAV swarm with n number of agents in R^3 under assumptions 1–3, where the positions and velocities of leader agents are time-varying. Based upon relative bearing measurements g_{ij} , relative distance measurements such as d_{ij} , and relative velocity measurements $v_{ij}(t)$, design an acceleration input $u_i(t)$ for each agent such that $g_{ij}^i(t) \rightarrow g_{ij}^*$ exponentially as $t \rightarrow \infty, \forall_i = 1, 2, \dots, n$.

Assumption 1. In this work, we assume that all UAVs are equipped with sensor packages, such as onboard-calibrated vision-based sensors, rate gyroscopes, accelerometers, and magnetometers, for accurate orientation calculation and also with communication modules to communicate with neighboring UAVs.

Assumption 2. Only the leader agent has the right to use the inertial reference frame; therefore, we assume other agents do not have this information. Another limitation on the leader agent is that it can only use that data to calculate its attitude in Euclidean space.

Problem 2. Consider a UAV swarm with n number of agents in R^3 with $\{p(0)\}_{i \in V}$ as initial positions and $\{Q(0)\}_{i \in V}$ as initial orientations under assumptions 1–2, and design an attitude synchronization law based on control inputs based on relative attitude and angular velocities of agents such that $\{q_{ij}(t)\}_{i \in V} \rightarrow 0, q_i \rightarrow q_j$ and $\omega_i \rightarrow \omega_j$ exponentially as $t \rightarrow \infty, \forall_i = 1, 2, \dots, n$.

3. Proposed Control Scheme

We designed a control scheme utilizing the information from both bearing and attitude controllers to control a swarm of quadcopter UAVs to form a specific formation shape, translate, and scale in 3D Euclidean space.

Figure 3 illustrates the block diagram of the proposed control structure depicting the flow of control inputs and outputs as well as their interaction with both controllers. The overall architecture of the control scheme and the designated operations of all UAVs are depicted in Figure 4.

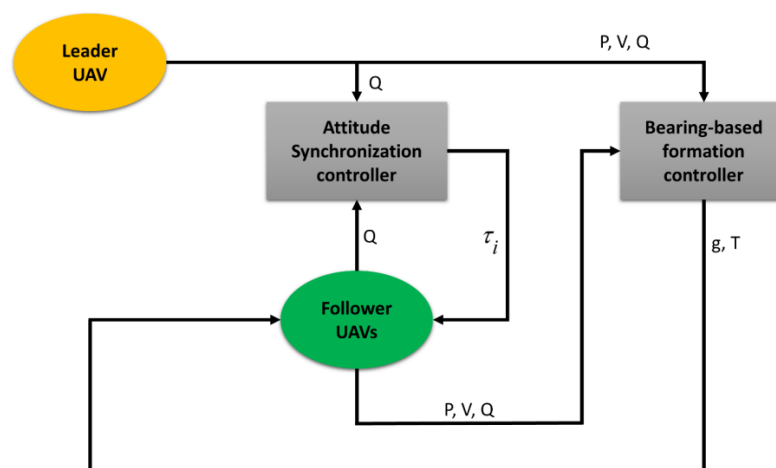


Figure 3. Block Diagram of Proposed Structure.

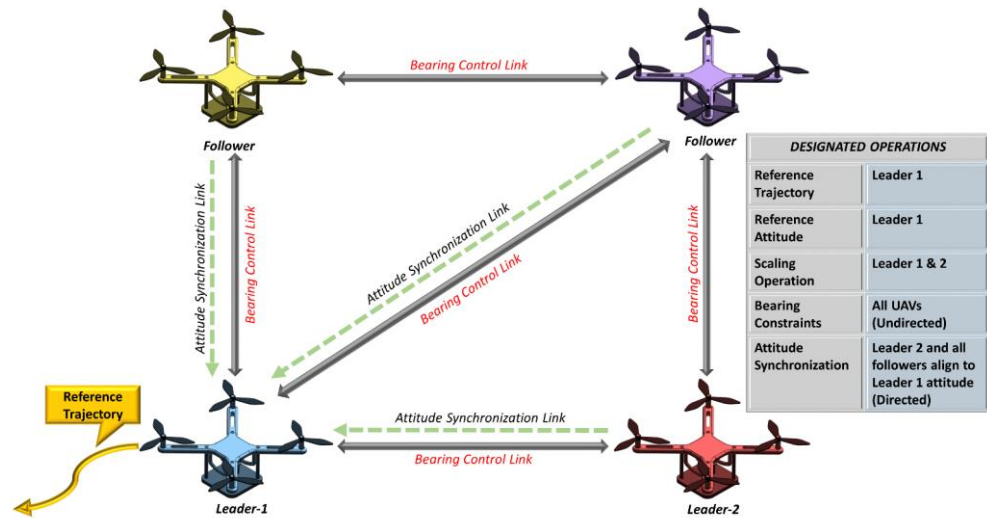


Figure 4. Overall Architecture and Designated Operations.

The interaction between each UAV, the flow of information, and designed operational tasks of all UAVs in a distributed manner are also explained in Figure 4. The formation was designed in such a way that each agent in the formation aligns itself with the spawned body frame of the leader agent. All control actions in 3D space such as formation acquisition, translation, scaling, and rotation were achieved by employing both controllers in unison. Therefore, bearing control and attitude synchronization were achieved in seamless harmony.

3.1. Bearing-Based Controller

To compute relative bearing between quadrotors in Euclidean space, considering assumptions 1–2, the position and velocity errors of agents are given as

$$\delta_p(t) = p_i(t) - p_i^*(t), \delta_v(t) = v_i(t) - v_i^*(t) \tag{21}$$

Given problem 1, the control objective was to design a control law for all agents in formation to make the complete formation do translational, rotational, and scaling maneuvers by enforcing $\delta_p(t) \rightarrow 0$ and $\delta_v(t) \rightarrow 0$ as $t \rightarrow \infty, \forall i = 1, 2, \dots, n$. It should be noted that only leaders know the desired translational, rotational, and scaling maneuvering information.

To accomplish the control objective, we propose a control structure where the target formation is tracked with time-varying velocity and time-varying orientation leaders. In this sub-section, we only consider the case of time-varying velocity leaders, and in the following sub-section (attitude controller), we consider the time-varying orientation leaders. According to [26], when the leader’s velocity $v_1(t)$ is time-varying, formation tracking errors might not converge to zero; therefore, a supplementary acceleration feedback term is required to be added in the controller. The following controller is proposed for the time-varying velocity leader case

$$u_i = -\xi_i^{-1} \sum_{j \in N_i} P_{g_{ij}^*} [k_p(p_i - p_j) + k_v(v_i - v_j) - \dot{v}_j] \tag{22}$$

where $\xi_i = \sum_{j \in N_i} P_{g_{ij}^*}$ and $P_{g_{ij}^*} = I_d - g_{ij}^* (g_{ij}^*)^T$ was defined earlier as an orthogonal projection matrix, while k_p and k_v are position and velocity positive control gains, respectively, and \dot{v}_j is the acceleration of the neighboring agent. The controller in (22) was inspired by consensus algorithms proposed in [39]. It can be proved that ξ_i is non-singular because the target formation to be tracked is unique.

Lemma 1. *The constant matrix ξ_i is non-singular for all follower agents if the acquired formation is distinct and unique.*

Proof of Lemma 1. Firstly, the matrix ξ_i is singular when the bearings g_{ij}^* are aligned because for any $x \in \mathbb{R}^d, x^T \xi_i x = 0 \Leftrightarrow \sum_{j \in N_i} x^T P_{g_{ij}^*} x = 0 \Leftrightarrow P_{g_{ij}^*} x = 0, \forall j \in N_i$. $\text{Null}(P_{g_{ij}^*}) = \text{span}\{g_{ij}^*\}$; therefore, $x^T \xi_i x = 0$ when x and g_{ij}^* are aligned. If g_{ij}^* is aligned, the follower position p_i^* cannot be estimated because p_i^* moves on the straight line aligned with g_{ij}^* . Resultantly, it can be established that ξ_i is singular. The stability analysis of control law (22) is given; hereby, \square

Theorem 1. *For the time-varying velocity leader, the position and velocity errors defined in (21) converge exponentially to zero.*

Proof of Theorem 1. Multiply ξ_i on both hand sides of the control law (22). $u_i = \dot{v}_i$; therefore,

$$\begin{aligned} \xi_i(\dot{v}_i - \dot{v}_j) &= \xi_i \xi_i^{-1} \sum_{j \in N_i} P_{g_{ij}^*} [-k_p(p_i - p_j) - k_v(v_i - v_j)] \\ \sum_{j \in N_i} P_{g_{ij}^*}(\dot{v}_i - \dot{v}_j) &= \sum_{j \in N_i} P_{g_{ij}^*} [-k_p(p_i - p_j) - k_v(v_i - v_j)] \end{aligned} \tag{23}$$

In terms of the bearing Laplacian matrix form,

$$\begin{aligned} B_{FF} \dot{v}_F + B_{FL} \dot{v}_L &= -k_p(B_{FF} P_F + B_{FL} P_L) - k_v(B_{FF} v_F + B_{FL} v_L) \\ &= -k_p B_{FF} \delta_p - k_v B_{FF} \delta_v \end{aligned} \tag{24}$$

With this, it can be shown that $\dot{v}_F = -k_p \delta_p - k_v \delta_v - B_{FF}^{-1} B_{FL} \dot{v}_L$, and therefore, the error terms are $\dot{\delta}_p = \dot{\delta}_v$ and $\dot{\delta}_v = \dot{v}_F + B_{FF}^{-1} B_{FL} \dot{v}_L = -k_p \delta_p + k_v \delta_v$, which can be shown in state space form as

$$\begin{bmatrix} \dot{\delta}_p \\ \dot{\delta}_v \end{bmatrix} = \begin{bmatrix} 0 & I \\ -k_p I & -k_v I \end{bmatrix} \begin{bmatrix} \delta_p \\ \delta_v \end{bmatrix} \tag{25}$$

The eigenvalue of this state matrix is $\lambda = (-k_v \pm \sqrt{k_v^2 \pm 4k_p})/2$, which proves to be in the left-half plane for any $k_p, k_v > 0$. Therefore, convergence is achieved. \square

3.2. Attitude Synchronization Controller

The orientation of follower UAVs is determined with respect to the orientation of the leader agent. As per problem 2, our objective was to guarantee attitude synchronization when $\omega_{ij} \rightarrow 0, Q_{ij} \rightarrow \pm Q_I$ and $R(Q_{ij}) \rightarrow I_3 \forall i, j \in N$. As $Q_{ij} = (q_{ij}^T \ \eta_{ij})^T$ is a unit vector representing the attitude from the i th agent (leader) and j th agent (follower), its inverse or conjugate can be written as

$$Q_{ij}^{-1} = \begin{pmatrix} -q_{ij} \\ \eta \end{pmatrix} \tag{26}$$

such that

$$Q_{ij} \odot Q_{ij}^{-1} = Q_{ij}^{-1} \odot Q_{ij} = Q_I \tag{27}$$

where Q_I is the unit quaternion identity and can be expressed as

$$Q_I = \begin{bmatrix} 0_3 \\ I \end{bmatrix} \tag{28}$$

Similarly, it can be seen that $R(Q_{ij}^{-1}) = R(Q_{ij})^T$. It is adequate to say that when $q_{ij} \rightarrow 0$, it implies that the attitude synchronization or alignment between agents has taken place. Furthermore, the relative attitude approximation is based on special orthogonal groups $SO(3)$, which guarantees accurate approximation for all UAVs in the formation. For translation of a UAV swarm in 3D space, the UAVs must track a reference trajectory; therefore, it is necessary to define an attitude tracking error. To do this, we define the desired attitude $Q_d = (q_d^T \quad \eta_d)^T$ with components of the unit quaternion described as

$$\dot{Q}_d = \frac{1}{2}T(Q_d)\omega_d \quad (29)$$

where $T(Q_d)$ is defined similarly to Equation (9). The attitude tracking error $\tilde{Q}_i = (\tilde{q}_i^T \quad \tilde{\eta}_i)^T$ can be defined as

$$\tilde{Q}_i = Q_d^{-1} \odot Q_i \quad (30)$$

Therefore, the relative attitude tracking can be written similarly to equation (11) as

$$\dot{\tilde{Q}}_i = \frac{1}{2}T(\tilde{Q}_i)\tilde{\omega}_i, \quad T(\tilde{Q}_i) = \begin{pmatrix} \tilde{\eta}_i I_3 + S(\tilde{q}_i) \\ -\tilde{q}_i^T \end{pmatrix} \quad (31)$$

where the angular velocity tracking vector can be defined as

$$\tilde{\omega}_i = \omega_i - R(\tilde{Q}_i)\omega_d \quad (32)$$

The rotation matrix associated to \tilde{Q}_i is given as

$$R(\tilde{Q}_i) = R(Q_i)R(Q_d)^T \quad (33)$$

For attitude synchronization and alignment of all UAVs in the swarm, the control input of each UAV has to be based upon relative attitudes and relative angular velocities among neighboring agents. Inspired by [40] and with the aim that all UAVs in the swarm align their attitudes and angular velocities in an undirected graph, the following attitude synchronization controller is proposed

$$\tau_i = \omega_i \times J_i \omega_i - J_i \sum_{j=1}^n a_{ij} [k_q q_{ij} + k_\omega (\omega_i - \omega_j)] \quad (34)$$

where a_{ij} is the value of a weighted adjacency matrix representing information exchange between UAVs, k_q and k_ω are positive scalar gains, and the value of inertia matrices $J \in \mathbb{R}^{3 \times 3}$ should be known for all UAVs in the swarm, which means that the controller can be implemented on heterogeneous quadcopter UAV swarms.

Theorem 2. For a time-varying orientation leader under the action of control law (34), the relative attitude and angular velocity between two neighboring UAVs should reach $q_{ij} \rightarrow 0$, $q_i \rightarrow q_j$, and $\omega_i \rightarrow \omega_j$ asymptotically as $t \rightarrow \infty$, $\forall i = 1, 2, \dots, n$.

Proof of Theorem 2. Select a Lyapunov candidate function, such as:

$$V = \frac{1}{2} \sum_{i=1}^n \sum_{j=1}^n a_{ij} k_{ij} \|q_{ij} - q_I\|^2 + \frac{1}{2} \sum_{i=1}^n \omega_i^T \omega_i \quad (35)$$

Under the dynamics of unit quaternions, the derivative of V becomes

$$\dot{V} = \frac{1}{2} \sum_{i=1}^n \sum_{j=1}^n a_{ij} k_{ij} (\omega_i - \omega_j)^T q_{ij} + \sum_{i=1}^n \omega_i^T (\tau_i - \omega_i \times J_i \omega_i) \tag{36}$$

As $\omega_i^T (\omega_i \times J_i \omega_i) = 0$, and under the fact that in an undirected graph $a_{ij} = a_{ji}$,

$$\begin{aligned} \dot{V} &= \frac{1}{2} \sum_{i=1}^n \sum_{j=1}^n a_{ij} k_{ij} (\omega_i - \omega_j)^T q_{ij} \\ &= \frac{1}{2} \sum_{i=1}^n \omega_i^T \left(\sum_{j=1}^n a_{ij} k_{ij} q_{ij} \right) - \frac{1}{2} \sum_{i=1}^n \sum_{j=1}^n a_{ij} k_{ij} \omega_j^T q_{ij} \\ &= \frac{1}{2} \sum_{i=1}^n \omega_i^T \left(\sum_{j=1}^n a_{ij} k_{ij} q_{ij} \right) - \frac{1}{2} \sum_{i=1}^n \sum_{j=1}^n a_{ji} k_{ji} \omega_j^T q_{ij} \\ &= \frac{1}{2} \sum_{i=1}^n \omega_i^T \left(\sum_{j=1}^n a_{ij} k_{ij} q_{ij} \right) + \frac{1}{2} \sum_{j=1}^n \sum_{i=1}^n a_{ji} k_{ji} \omega_j^T q_{ij} \\ &= \frac{1}{2} \sum_{i=1}^n \omega_i^T \left(\sum_{j=1}^n a_{ij} k_{ij} q_{ij} \right) + \frac{1}{2} \sum_{j=1}^n \omega_j^T \left(\sum_{i=1}^n a_{ji} k_{ji} q_{ij} \right) \\ &= \sum_{i=1}^n \omega_i^T \left(\sum_{j=1}^n a_{ij} k_{ij} q_{ij} \right) \end{aligned} \tag{37}$$

Resultantly, Equation (36) becomes

$$\dot{V} = \sum_{i=1}^n \omega_i^T \left(\sum_{j=1}^n a_{ij} k_{ij} q_{ij} + \tau_i \right) \tag{38}$$

$\sum_{i=1}^n \omega_i^T \sum_{j=1}^n a_{ij} k_{ij} (\omega_i - \omega_j) = \frac{1}{2} \sum_{i=1}^n \sum_{j=1}^n a_{ij} k_{ij} \| \omega_i - \omega_j \|^2$; therefore, the derivative of V becomes negative semidefinite

$$\dot{V} = - \frac{1}{2} \sum_{i=1}^n \sum_{j=1}^n a_{ij} k_{ij} \| \omega_i - \omega_j \|^2 \leq 0 \tag{39}$$

By LaSalle’s invariance principle, it is established that $q_{ij} \rightarrow 0$, $q_i \rightarrow q_j$, and $\omega_i \rightarrow \omega_j$ asymptotically. □

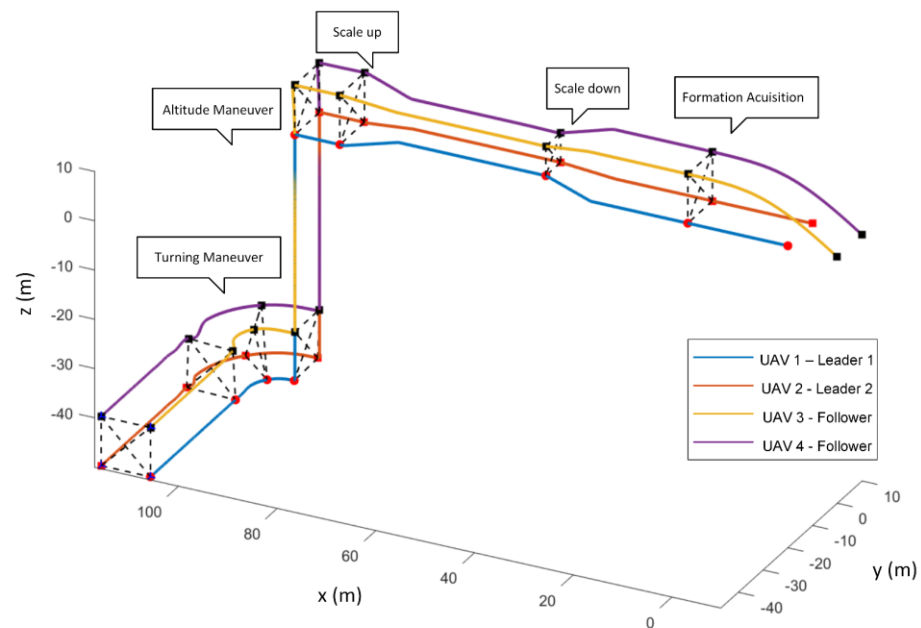
4. Simulation Results

In this section, we share numerical simulation results demonstrating the effectiveness of our proposed model on a swarm of quadrotor UAVs. This swarm of UAVs contained four quadrotors depicting an undirected leader–follower topology. The formation consisted of two leaders and two follower UAVs. To highlight the operations of the formation in a simple way, a square-shaped geometric configuration was selected, and the communication topology is described in Figure 3, which depicts leader agents as $V_L = \{1, 2\}$ and followers as $V_F = \{3, 4\}$. The model information and specifications are given in Table 1.

In this work, we assumed that the formation encounters various kinds of obstacles in its path while translating in an underground environment, e.g., narrow passages, pipes, tunnels, etc., and negotiates those obstacles while keeping the formation intact. Figure 5 depicts the entire time-lapse of the formation translation and different maneuvers. The formation was designed to carry out four distinct actions, and the case-wise details of all actions and maneuvers achieved by the formation are given below.

Table 1. Model Information and specifications.

Parameter	Value
m	0.80
$J(\text{kgm}^2)$	$[1,0,1,0,1; 0,1,0,1,0,1; 0,1,0,1,0,9]$
a_{ij}	$[0,1,1,1; 1,0,1,1; 1,1,0,1; 1,1,1,0]$
k_q	1
k_ω	10
k_p	0.5
k_v	2

**Figure 5.** Time-lapse of complete formation operation.

4.1. Case 1—Formation Acquisition

- (1) Objective: a swarm of four UAVs at random positions takes off and acquires a specific square shape under the control of proposed laws.
- (2) Results: the target formation formed a designated square shape and was attained by implementing pre-defined bearing constraints between the agents as $g_{21}^* = -g_{12}^{*T}$, $g_{31}^* = -g_{13}^*$, $g_{12}^* = [-1 \ 0 \ 0]^T$, $g_{13}^* = [0 \ 0 \ -1]^T$, $g_{14}^* = \left[\frac{-\sqrt{2}}{2} \ 0 \ \frac{-\sqrt{2}}{2} \right]^T$, $g_{41}^* = -g_{14}^*$, $g_{23}^* = \left[\frac{\sqrt{2}}{2} \ 0 \ \frac{-\sqrt{2}}{2} \right]^T$, $g_{32}^* = -g_{23}^*$, $g_{42}^* = [0 \ 0 \ 1]^T$, and $g_{24}^* = -g_{42}^*$. The formation trajectories are given in Figure 5. The formation tracking error $\|\delta_i\|$ is shown in Figure 6 (section highlighted in blue), which asymptotically converged to zero from $t = 0$ to 20 s.

4.2. Case 2—Formation Scaling

- (1) Objective: to verify that formation can scale down (decrease size) and scale up (increase size) while translating in 3D space by still keeping formation-bearing constraints, inter-agent distances, and heading direction intact.
- (2) Results: the formation continued translation on the x -axis, scaled down at $t = 40$ s, and scaled up at $t = 80$ s to negotiate imaginary obstacles. This was achieved by adjusting and altering the distance and velocities of two leaders. Figure 5 depicts both scaling operations, and Figure 6 shows the convergence of formation tracking errors to zero (highlighted with yellow color for scaling down and with green color for scaling up).

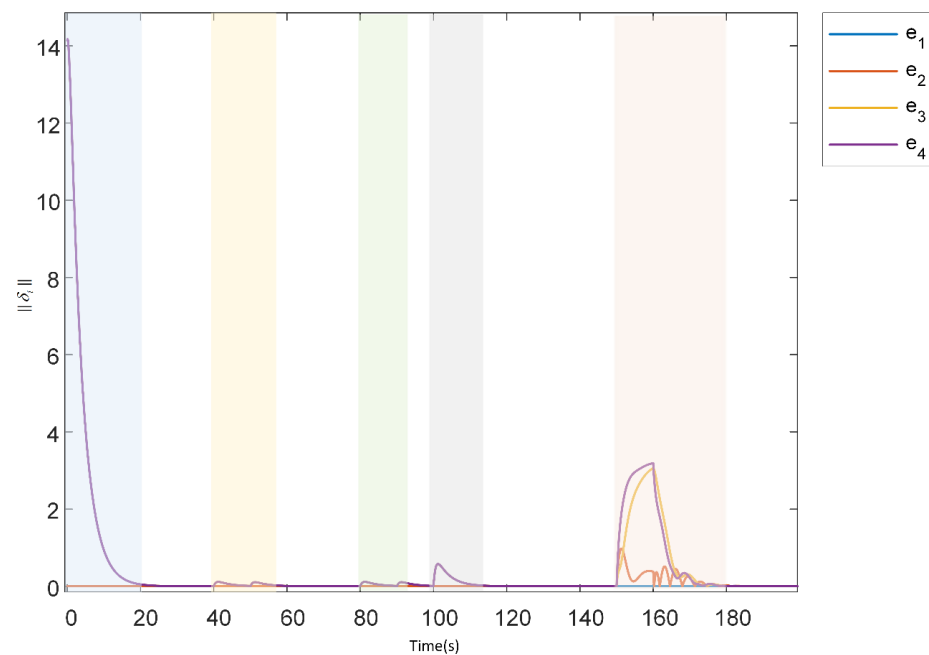


Figure 6. Formation tracking errors.

4.3. Case 3—Altitude Maneuver

- (1) Objective: to verify that UAVs in the formation can also make an altitude descent while staying in the desired formation to negotiate an obstacle or follow a specific trajectory involving sudden altitude descent.
- (2) Results: after the scaling operation while translating in the x -axis direction, the formation abruptly descended its altitude in the z -axis direction in 3D space at $t = 100$ to 110 s by altering the velocity of leaders. The trajectory plot of UAVs is given in Figure 5, and the formation tracking error converged to zero asymptotically as shown in Figure 6 (highlighted with grey color).

4.4. Case 4—Formation Translational Rotation

- (1) Objective: to verify that formation while translating in 3D space can rotate its heading direction by altering the velocity of agents such that the swarm stays dynamically intact.
- (2) Results: in Figure 5 at $t = 150$ to 180 s, it can be seen that the final formation was rotated from the initial formation heading direction by altering the leader's orientation so that the formation takes a translational rotation. The formation tracking error also converged to zero as shown in Figure 6 (section highlighted in orange color).

Both the bearing-based controller and attitude controller ensured the performance of the formation during the entirety of the operation. The attitude controller aligned the attitude of all follower UAVs as per the attitude of leader UAVs at every stage of formation operation as shown in Figure 7. As can be seen in the figures, the different cases of formation operations are shown at different time intervals such as formation acquisition ($t = 0$ to 20 s), scale-down ($t = 0$ to 20 s), scale-up ($t = 0$ to 20 s), altitude descend ($t = 0$ to 20 s) and translation maneuver ($t = 0$ to 20 s).

The linear velocity of all follower UAVs achieved consensus as per the linear velocity of the leader UAV, as shown in Figure 8 for all cases. Figure 8a,b illustrates the linear velocity profile of all agents in the x and y -axis where it can be noticed that Leader-2 (agent 2) had the maximum deviation; this is because as per configuration, agent 2 lay at the farthest end and had to align itself with the rest of the agents. Therefore, the controller action forced agent 2 to rapidly align with the rest of the formation, ensuring the formation configuration is intact. Similarly, in Figure 8c, it can be noticed that the velocity profile of agents 1 and 2 and agents 3 and 4 were identical; this is because of the formation configuration as can be

seen in Figure 5. The angular velocity of all followers converged to that of the leader UAV, as can be seen in Figure 9 for all cases, while the formation tracking error remained at zero despite the hard inclination in maneuvers.

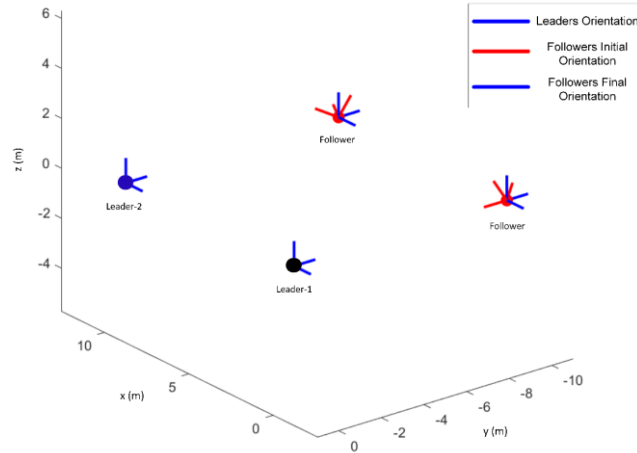


Figure 7. Attitude synchronization.

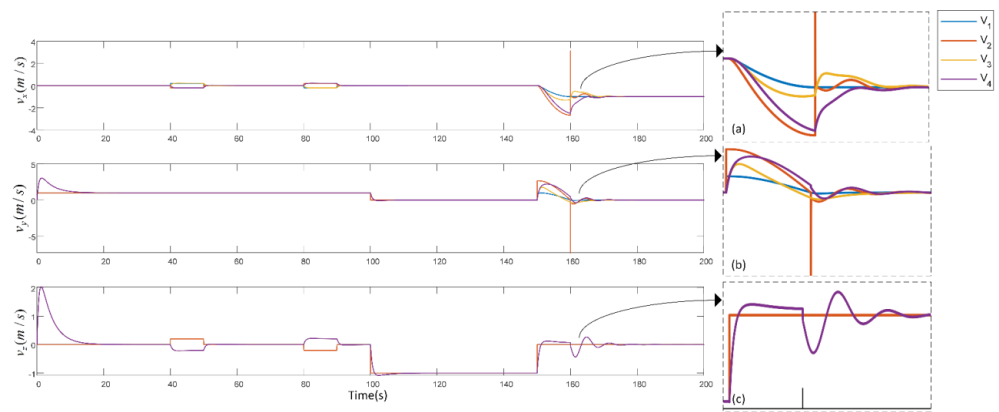


Figure 8. Linear velocity profile. (a) Magnified view of velocity peaks in x-axis at t = 160 s. (b) Magnified view of velocity peaks in y-axis at t=160 s. (c) Magnified view of velocity peaks in z-axis at t = 160 s.

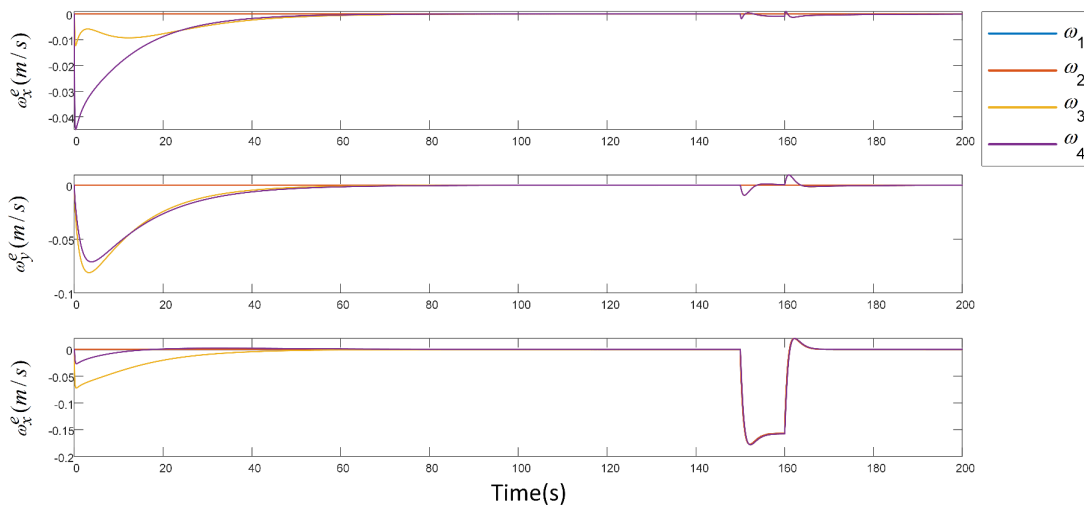


Figure 9. Angular velocity profile.

The orientation of the leader is time-varying because of changing maneuvers; therefore, in Figure 10, it can be seen that all followers aligned their orientation to that of the leader as per changing maneuvers; hence, the attitude error was maintained at zero. The same is represented in Figure 11 in terms of roll, pitch, and yaw angles.

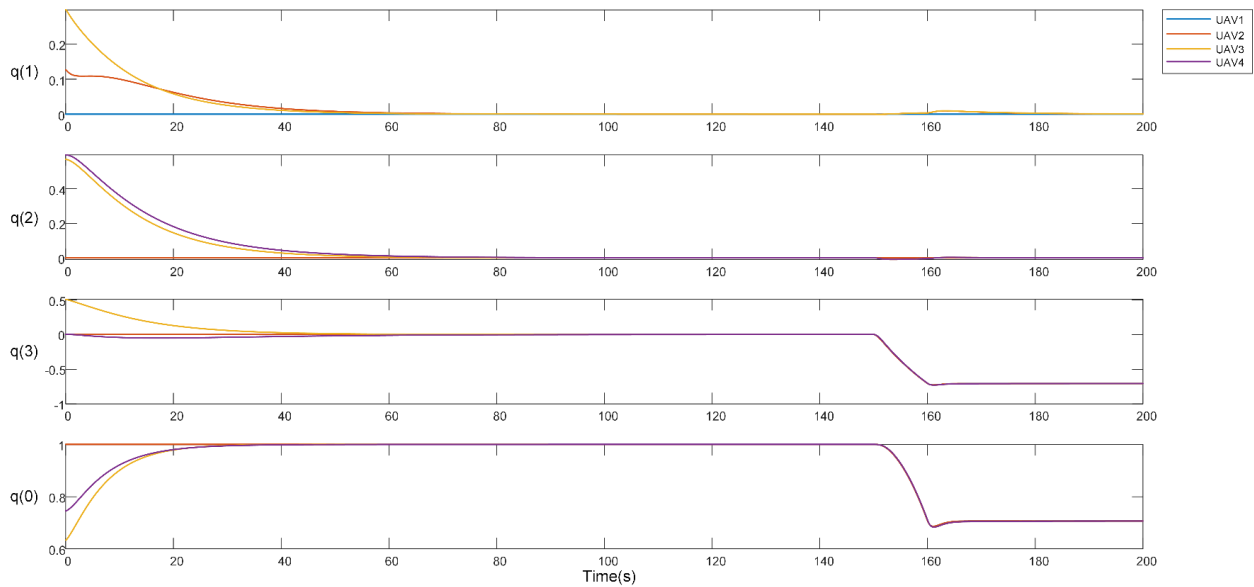


Figure 10. Attitude synchronization in quaternions.

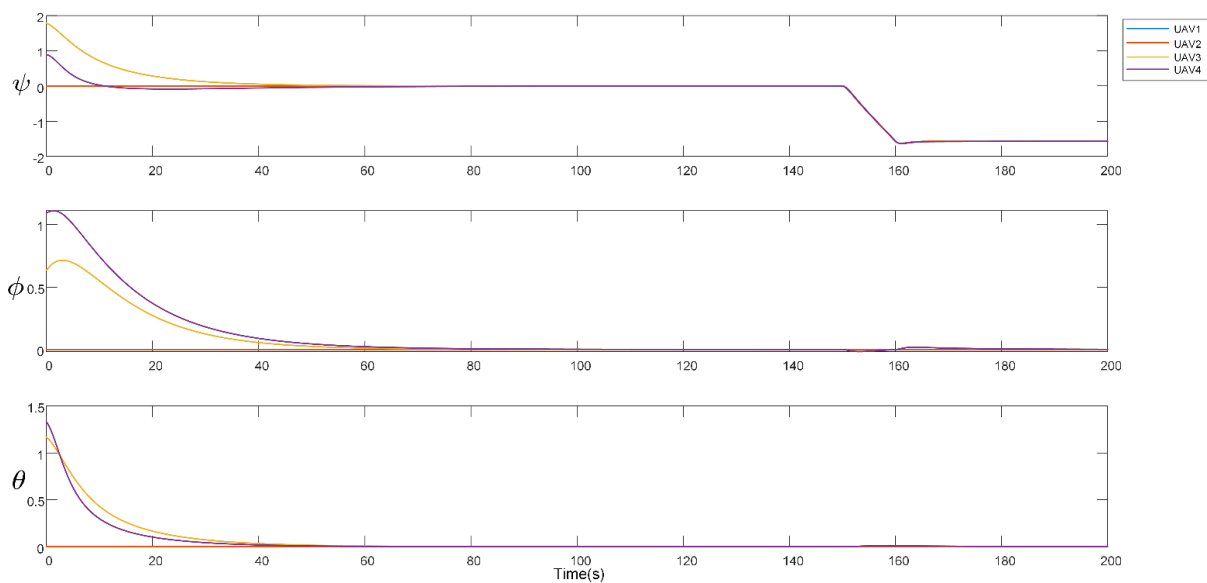


Figure 11. Attitude synchronization as per yaw, pitch, and roll angles.

5. Discussion

From the results of the case studies and simulations above, it can be established that the formation carried out the specified tasks efficiently. The leader aligned its body frame with the inertial reference frame and moved in the 3D Euclidean space without any further constraints while followers followed the leaders as per the designed topology. All UAVs in the swarm were responsible for maintaining bearing vectors; hence, the desired formation and maneuvers were done in an undirected manner. The formation could avoid narrow obstacles and pass through tight corners and obstacles because the scale, orientation, translation, and velocity could be adjusted. Moreover, the attitude synchronization controller was designed in such a way that it can be implemented not only on homogeneous quadrotor

formations but can also support heterogeneous quadrotor formations. For bearing-based UAV formation control problems, the orientation parameters are often neglected or calculated using a primary de facto method of Euler angles for attitude representation. The quaternion-based orientation approximation provides robust, unambiguous, and computationally efficient attitude calculation. Attitude calculations by quaternions ensure that agents in the swarm do not suffer from gimbal lock and singularities, improving the control scheme's overall robustness. Calculating attitude and bearing in the local body frames of each agent is advantageous because agents do not have to depend on the global frame, as GPS signals may be faulty in subterranean environments (e.g., indoors, underwater, deep space, etc.). Many previous works such as [31,41] have assumed that the body frame of the UAV should coincide with the center of mass, while we suggested that it should coincide at the geometrical center of the UAV for accurate position and orientation measurement.

6. Conclusions

This work investigated the joint operation of bearing-based and attitude synchronization controllers to control a quadcopter UAV swarm in 3D space by using undirected graph topology. This combination of controllers added to the overall robustness of formation during complicated maneuvers. Since this work focused on the distributed formation control by depicting various motions of the formation in 3D space, its limitation is that obstacle avoidance was not considered during practical implementation. Further performance improvement for more complex maneuvers such as curved trajectories and implementation of this work on experimental platforms are treated as future works.

Author Contributions: Conceptualization, M.B.S. and Y.Z.; methodology, M.B.S. and Y.Z.; software, M.B.S. and Z.Y.; investigation, X.W. and X.Y.; writing—original draft preparation, M.B.S. and Z.L.; writing—review and editing, M.B.S. and S.A.; supervision, S.W. All authors have read and agreed to the published version of the manuscript.

Funding: This study was co-supported by the National Science and Technology Major Project of China (Nos. 2017-V-0010-0060, 2017-V-0011-0062), National Natural Science Foundation of China (Nos. 51675019, 51620105010), and the fellowship of China Postdoctoral Science Foundation (Grant No.2022M710305).

Institutional Review Board Statement: Not applicable.

Informed Consent Statement: Not applicable.

Data Availability Statement: Not applicable.

Acknowledgments: The authors would like to thank all the teachers at the School of Automation Science and Electrical Engineering, Beihang University for their support and advice in the completion of this work.

Conflicts of Interest: The authors declare no conflict of interest.

References

1. Bai, H.; Wen, J.T. Cooperative Load Transport: A Formation-Control Perspective. *IEEE Trans. Robot.* **2010**, *26*, 742–750. [[CrossRef](#)]
2. Liu, G.P.; Zhang, S. A Survey on Formation Control of Small Satellites. *Proc. IEEE* **2018**, *106*, 440–457. [[CrossRef](#)]
3. Dong, X.; Zhou, Y.; Ren, Z.; Zhong, Y. Time-Varying Formation Tracking for Second-Order Multi-Agent Systems Subjected to Switching Topologies With Application to Quadrotor Formation Flying. *IEEE Trans. Ind. Electron.* **2017**, *64*, 5014–5024. [[CrossRef](#)]
4. Zhang, J.; Xing, J. Cooperative Task Assignment of Multi-UAV System. *Chin. J. Aeronaut.* **2020**, *33*, 2825–2827. [[CrossRef](#)]
5. Wang, Y.; Zhang, T.; Cai, Z.; Zhao, J.; Wu, K. Multi-UAV Coordination Control by Chaotic Grey Wolf Optimization Based Distributed MPC with Event-Triggered Strategy. *Chin. J. Aeronaut.* **2020**, *33*, 2877–2897. [[CrossRef](#)]
6. Zhen, Z.; Zhu, P.; Xue, Y.; Ji, Y. Distributed Intelligent Self-Organized Mission Planning of Multi-UAV for Dynamic Targets Cooperative Search-Attack. *Chin. J. Aeronaut.* **2019**, *32*, 2706–2716. [[CrossRef](#)]
7. Zhang, P.; De Queiroz, M.; Cai, X. Three-Dimensional Dynamic Formation Control of Multi-Agent Systems Using Rigid Graphs. *J. Dyn. Syst. Meas. Control Trans. ASME* **2015**, *137*, 111006. [[CrossRef](#)]
8. Sial, M.B.; Wang, S.; Wang, X.; Wyrwa, J.; Liao, Z.; Ding, W. Mission Oriented Flocking and Distributed Formation Control of UAVs. In Proceedings of the 16th IEEE Conference on Industrial Electronics and Applications, ICIEA 2021, Chengdu, China, 1–4 August 2021.

9. Oh, K.K.; Park, M.C.; Ahn, H.S. A Survey of Multi-Agent Formation Control. *Automatica* **2015**, *53*, 424–440. [[CrossRef](#)]
10. Lin, Z.; Ding, W.; Yan, G.; Yu, C.; Giua, A. Leader-Follower Formation via Complex Laplacian. *Automatica* **2013**, *49*, 1900–1906. [[CrossRef](#)]
11. Lewis, M.A.; Tan, K.H. High Precision Formation Control of Mobile Robots Using Virtual Structures. *Auton. Robot.* **1997**, *4*, 387–403. [[CrossRef](#)]
12. Hsieh, M.A.; Kumar, V.; Chaimowicz, L. Decentralized Controllers for Shape Generation with Robotic Swarms. *Robotica* **2008**, *26*, 691–701. [[CrossRef](#)]
13. Mesbahi, M.; Egerstedt, M. *Graph Theoretic Methods in Multiagent Networks*; Princeton University Press: Princeton, NJ, USA, 2010.
14. Giribet, J.I.; Colombo, L.J.; Moreno, P.; Mas, I.; Dimarogonas, D.V. Dual Quaternion Cluster-Space Formation Control. *IEEE Robot. Autom. Lett.* **2021**, *6*, 6789–6796. [[CrossRef](#)]
15. CAI, Z.; WANG, L.; ZHAO, J.; WU, K.; WANG, Y. Virtual Target Guidance-Based Distributed Model Predictive Control for Formation Control of Multiple UAVs. *Chin. J. Aeronaut.* **2020**, *33*, 1037–1056. [[CrossRef](#)]
16. Zou, Y.; Zhou, Z.; Dong, X.; Meng, Z. Distributed Formation Control for Multiple Vertical Takeoff and Landing UAVs with Switching Topologies. *IEEE/ASME Trans. Mechatron.* **2018**, *23*, 1750–1761. [[CrossRef](#)]
17. CHEN, H.; WANG, X.; SHEN, L.; CONG, Y. Formation Flight of Fixed-Wing UAV Swarms: A Group-Based Hierarchical Approach. *Chin. J. Aeronaut.* **2021**, *34*, 504–515. [[CrossRef](#)]
18. Trinh, M.H.; Pham, V.H.; Park, M.C.; Sun, Z.; Anderson, B.D.O.; Ahn, H.S. Comments on “Global Stabilization of Rigid Formations in the Plane [Automatica 49 (2013) 1436–1441]”. *Automatica* **2017**, *77*, 393–396. [[CrossRef](#)]
19. Mou, S.; Belabbas, M.A.; Morse, A.S.; Sun, Z.; Anderson, B.D.O. Undirected Rigid Formations Are Problematic. *IEEE Trans. Automat. Contr.* **2016**, *61*, 2821–2836. [[CrossRef](#)]
20. Cai, X.; Queiroz, M. De Adaptive Rigidity-Based Formation Control for Multirobotic Vehicles with Dynamics. *IEEE Trans. Control Syst. Technol.* **2015**, *23*, 389–396. [[CrossRef](#)]
21. Li, X.; Wen, C.; Chen, C. Adaptive Formation Control of Networked Robotic Systems with Bearing-Only Measurements. *IEEE Trans. Cybern.* **2021**, *51*, 199–209. [[CrossRef](#)]
22. Zhao, S.; Lin, F.; Peng, K.; Chen, B.M.; Lee, T.H. Distributed Control of Angle-Constrained Cyclic Formations Using Bearing-Only Measurements. *Syst. Control Lett.* **2014**, *63*, 12–24. [[CrossRef](#)]
23. Basiri, M.; Bishop, A.N.; Jensfelt, P. Distributed Control of Triangular Formations with Angle-Only Constraints. *Syst. Control Lett.* **2010**, *59*, 147–154. [[CrossRef](#)]
24. Zhao, S.; Zelazo, D. Bearing Rigidity and Almost Global Bearing-Only Formation Stabilization. *IEEE Trans. Automat. Contr.* **2016**, *61*, 1255–1268. [[CrossRef](#)]
25. Li, Z.; Tnunay, H.; Zhao, S.; Meng, W.; Xie, S.Q.; Ding, Z. Bearing-Only Formation Control With Prespecified Convergence Time. *IEEE Trans. Cybern.* **2020**, *52*, 620–629. [[CrossRef](#)]
26. Zhao, S.; Zelazo, D. Translational and Scaling Formation Maneuver Control via a Bearing-Based Approach. *IEEE Trans. Control Netw. Syst.* **2017**, *4*, 429–438. [[CrossRef](#)]
27. Tron, R.; Thomas, J.; Loianno, G.; Daniilidis, K.; Kumar, V. A Distributed Optimization Framework for Localization and Formation Control: Applications to Vision-Based Measurements. *IEEE Control Syst.* **2016**, *36*, 22–44. [[CrossRef](#)]
28. Gurbuz, A.C.; Cevher, V.; McClellan, J.H. Bearing Estimation via Spatial Sparsity Using Compressive Sensing. *IEEE Trans. Aerosp. Electron. Syst.* **2012**, *48*, 1358–1369. [[CrossRef](#)]
29. Chen, Y.M.; Lee, J.H.; Yeh, C.C.; Mar, J. Bearing Estimation Without Calibration for Randomly Perturbed Arrays. *IEEE Trans. Signal Process.* **1991**, *39*, 194–197. [[CrossRef](#)]
30. Carino, J.; Abaunza, H.; Castillo, P. Quadrotor Quaternion Control. In Proceedings of the 2015 International Conference on Unmanned Aircraft Systems, ICUAS 2015, Denver, Colorado, USA, 9–12 June 2015.
31. Zhang, Y.; Wang, X.; Wang, S.; Tian, X. Distributed Bearing-Based Formation Control of Unmanned Aerial Vehicle Swarm via Global Orientation Estimation. *Chin. J. Aeronaut.* **2021**, *35*, 44–58. [[CrossRef](#)]
32. Goldstein, H.; Poole, P.C.; Safko, J.L. *Pearson Education—Classical Mechanics*; Pearson: London, UK, 2002.
33. Dantam, N.T. Robust and Efficient Forward, Differential, and Inverse Kinematics Using Dual Quaternions. *Int. J. Rob. Res.* **2021**, *40*, 1087–1105. [[CrossRef](#)]
34. Qiuling, J.; Guangwen, L.; Jingchao, L. Formation Control and Attitude Cooperative Control of Multiple Rigid Body Systems. In Proceedings of the ISDA 2006: Sixth International Conference on Intelligent Systems Design and Applications, Jinan, China, 16–18 October 2006; Volume 2.
35. Wang, P.K.C.; Hadaegh, F.Y.; Lau, K. Synchronized Formation Rotation and Attitude Control of Multiple Free-Flying Spacecraft. *J. Guid. Control Dyn.* **1999**, *22*, 28–35. [[CrossRef](#)]
36. Abdelkader Abdessameud, A.T. *Motion Coordination for VTOL Unmanned Aerial Vehicles: Attitude Synchronisation and Formation Control*; Springer Science & Business Media: Berlin/Heidelberg, Germany, 2013.
37. Zhao, S.; Zelazo, D. Bearing Rigidity Theory and Its Applications for Control and Estimation of Network Systems: Life beyond Distance Rigidity. *IEEE Control Syst.* **2019**, *39*, 66–83. [[CrossRef](#)]
38. Trinh, M.H.; Zhao, S.; Sun, Z.; Zelazo, D.; Anderson, B.D.O.; Ahn, H.S. Bearing-Based Formation Control of a Group of Agents with Leader-First Follower Structure. *IEEE Trans. Automat. Contr.* **2019**, *64*, 598–613. [[CrossRef](#)]
39. Ren, W. On Consensus Algorithms for Double-Integrator Dynamics. *IEEE Trans. Automat. Contr.* **2008**, *53*, 1503–1509. [[CrossRef](#)]

-
40. Ren, W. Distributed Attitude Alignment in Spacecraft Formation Flying. *Int. J. Adapt. Control Signal Process.* **2007**, *21*, 95–113. [[CrossRef](#)]
 41. Huang, Y.; Meng, Z. Bearing-Based Distributed Formation Control of Multiple Vertical Take-Off and Landing UAVs. *IEEE Trans. Control Netw. Syst.* **2021**, *8*, 1281–1292. [[CrossRef](#)]